www.elsevier.com/locate/talanta

Simple and label-free detection of DNA hybridization on a modified graphene nanosheets electrode

Ali Benvidi, Nooshin Rajabzadeh, Hossein Molaye Zahedi, Mohammad Mazloum-Ardakani, Mohammad M. Heidari, Laleh Hosseinzadeh

PII: S0039-9140(15)00063-6
DOI: http://dx.doi.org/10.1016/j.talanta.2015.01.035
Reference: TAL15363

To appear in: *Talanta*

Received date: 1 November 2014
Revised date: 23 January 2015
Accepted date: 24 January 2015

Cite this article as: Ali Benvidi, Nooshin Rajabzadeh, Hossein Molaye Zahedi, Mohammad Mazloum-Ardakani, Mohammad M. Heidari, Laleh Hosseinzadeh, Simple and label-free detection of DNA hybridization on a modified graphene nanosheets electrode, *Talanta,* http://dx.doi.org/10.1016/j.talanta.2015.01.035

Simple and label-free detection of DNA hybridization on a modified graphene nanosheets electrode

Ali Benvidi[1,a], Nooshin Rajabzadeh[a], Hossein Molaye Zahedi[a], Mohammad Mazloum-Ardakani[a], Mohammad M. Heidari[b], Laleh Hosseinzadeh[a]

[a]*Department of Chemistry, Faculty of Science, Yazd University, Yazd 89195-741, Iran*

[b]*Department of Biology, Faculty of Science, Yazd University, Yazd 89195-741, Iran*

Abstract

In this study, an effective method was devised to synthesize of amelogenin genes in solution and to amplify electrical detection of DNA hybridization based on graphene nanosheets (GNs) modified glassy carbon electrode (GCE). GNs are well known as effective biocompatible and conductive materials that can provide large surface area and a sufficient numbers of binding points for DNA immobilization. The biosensor fabrication processes and the electrochemical responses of probe immobilization and hybridization with target DNA were investigated by electrochemical impedance spectroscopy (EIS) and cyclic voltammetry (CV) using $[Fe(CN)_6]^{3-/4-}$ as an electrochemical redox. Due to minimum nonspecific DNA adsorption, a very high specificity of DNA hybridization was achieved, and the hybridization rate of the target DNA in optimum conditions was increased significantly. With this approach, the target DNA could be quantified in a linear range from 1.0×10^{-20} to 1.0×10^{-14} mol L^{-1} for the first segment and from 1.0×10^{-13} to 1.0×10^{-6} mol L^{-1} for the second segment, with a detection limit of 7.1×10^{-21} mol L^{-1} by 3sb. In addition, the biosensor exhibited a high level of stability and repeatability, even for the determination of DNA sequences in real samples without amplification.

Keywords*:* DNA biosensor; DNA hybridization; Amelogenin gene; Graphene nanosheets; Electrochemical impedance spectroscopy

1. Introduction

*[1]Corresponding author: Tel.: +98 351 8122645; Fax: 98 351 8210644.

e-mail address: benvidi89@gmail.com, abenvidi@yazd.ac.ir,

DNA biosensors were employed for the detection of nucleic acid sequences have attracted increasing interests in connection with efforts directed to gene analysis, clinical disease diagnosis, and even forensic applications [1, 2]. Nucleic acid hybridization of single-stranded probes with targets has been increasingly used in various analytical strategies for the clinical laboratory testing of genetic and infectious diseases [3]. Different techniques including optical technique [4], quartz crystal microbalance [5], surface plasmon resonance spectroscopy [6], and electrochemistry [7-9] have been well developed for DNA detection. Considerable efforts have been made to develop methods for rapid detection of hybridization events. Among them, electrochemistry offers great advantages such as simplicity, low cost and high sensitivity [8]. One of the key issues in the use of any DNA hybridization biosensor is the rate of immobilization and accessibility of probe DNA for hybridization recognition [9]. Increasing the rate of immobilization and controlling the molecular orientation of probe DNA would markedly improve the performance properties of DNA biosensors. In order to achieve this goal, nanomaterials may be used as an excellent solution for the control of DNA immobilization. GNs have attracted much attention because of their intriguing crystalline, mechanical, and electronic properties, despite their short history of realization [10, 11]. GNs, as “a single layer of carbon atoms in a closely packed honey comb two-dimensional lattice”, were first reported in 2004 [12]. They have proved to be of potential applications in nanoelectronic devices due to their novel properties such as good mechanical strength, large specific surface area, and high conductivity [13]. Examples of these applications include transparent conductors [14], sensors [15], super capacitors [16], batteries, hydrogen storages [10] and nanocomposite materials [17]. However, the lack of an efficient approach to produce GNs in large quantities has been a major obstacle to exploit most proposed applications of these materials.

EIS is a method to analyze the electrical resistance of a system using equivalent circuits. This analytical method is highly sensitive to changes occurring on the electrode surface; therefore, EIS is an appropriate technique for DNA detection [18]. This technique is inherently a label-free detection method which is especially beneficial due to the fact that there is no need to additionally modify biomolecules with such markers as fluorescent dyes, enzymes, or other redox labels [19]. At the time of taking measurements with surface-modified electrodes, redox-active compounds are usually added to the electrolyte solution. If a redox-active compound is blocked by adding a blocking layer to the electrode, such as DNA attracted to a modified

electrode, the charge-transfer resistance (R_{ct}) value becomes larger. In addition, hybridization reaction of DNA on the electrode surface results in a change of the R_{ct} value. The quantity of the negative charge on the surface of the electrode increases greatly due to hybridization formation and further impeding of electron transfer.

Amelogenin is a major protein constituent of the developing enamel matrix. This protein is now well characterized, using the data of amino acid sequences, as to be of a high degree of homology among all species investigated to date. The gene structure of this protein has been demonstrated. It is confirmed that there are two amelogenin genes, one on the X-chromosome and the other on the Y-chromosome in humans. The physiological importance of amelogenin in enamel formation is suggested by the symptoms of this inherited disease in addition to the inhibition experiments of amelogenin transcription and translation [20].

In this research, a highly sensitive, facile, stable and label-free DNA biosensor was established based on GNs as a platform. In addition, for the rapid synthesis and detection of amelogenin gene hybridization, a favorable method was applied without polymerase chain reaction (PCR). This method of genosensing is a quick approach for synthesizing and detecting DNA without using additional label. The hybridization biosensor was fabricated by chemisorption of 17-mer oligonucleotide modified with an amine group at its 3´terminal. Immobilization process was performed in the presence of activators soluble in water 1-ethyl-3(3-dimethylaminopropyl)-carbodiimide (EDC) and N-hydroxysulfosuccinimide (NHS). Covalent immobilization of DNA on the electrode surface exhibits some advantages as compared to simple adsorption. This is mainly due to the fact that nucleic acid chains are bonded to an electrode surface by one end, which only ensures structural flexibility and increases hybridization without DNA leakage. The calibration curve showed a linear relationship with the target DNA concentrations in the range from 1.0×10^{-20} to 1.0×10^{-14} mol L^{-1} for the first segment and from 1.0×10^{-13} to 1.0×10^{-6} mol L^{-1} for the second segment, with the detection limit of 7.1×10^{-21} mol L^{-1}. In our previous paper, an electrochemical hybridization biosensor was introduced based on reduced graphene oxide. The detection limit in the proposed biosensor is as low as the one in our previous study (7.1×10^{-21} mol L^{-1} in the proposed method compared to 3.2×10^{-21} mol L^{-1} in the previous work). This is because the probe DNA molecules are spatially well arranged. Under optimal conditions, this biosensor can achieve a high sensitivity to detect real samples extracted from blood. Another advantage of the proposed biosensor is its wider

linear range. The synthesis of a nucleic acid copy (DNA) detected by electrochemical methods such as EIS is one of the novelties in this paper as compared with our previous study.

2. Experiment

2.1 Reagents

The probes were designed based on amelogenin gene obtained from the Gene Bank database. The oligonucleotides were designed by primer design software (Premier 5.0, Premier Biosoft, Canada), and their secondary structure was tested with Gene Runner (version 3.05, Hastings Software, USA). Deoxyribonucleotide triphosphate (dNTP) and Klenow enzyme (i.e. the large fragment of E. coli DNA polymerase I) were purchased from Sina Clone Company, Iran. Oligonucleotides (17mer probe and complementary target) were synthesized by Macrogen (Korea) and had the following sequences:

• Immobilized probe specific: 5'-CATCCCAAATAAAGTG- NH_2-3'
• Complementary sequence: 5'- CACTTTATTTGGGATG -3'
• Noncomplementary sequence: 5'- GAGAAACATCTGGGATA -3'

Chemical reagents including sodium dihydrogen phosphate, disodium hydrogen phosphate, EDC, NHS, 2-(N-morpholino) ethane sulfonic acid (MES buffer), Tween 20 (Polyoxyethylenesorbitan monolaurate), potassium ferrocyanide, potassium ferricyanide, graphite and hydrazine monohydrate (N_2H_4, 98%) were purchased from commercial sources (Merck or Sigma) in analytical grades. Ultrapure water was obtained from a water purification system (with resistivity of 18.2 MΩ cm^{-1}) and used in all the buffer solutions. The washing solution was a 0.05 M phosphate buffer (pH = 7.4) containing 0.3 mol L^{-1} of NaCl. The buffer solution was adjusted by adding NaOH or HCl solutions. The double distilled water and all the buffer solutions were sterilized using an autoclave. The stock solutions of the oligonucleotides (100.0 µmol L^{-1}) were prepared in 0.1 mol L^{-1} PBS solution (pH=7.4), and kept frozen at -20 °C.

2.2 Instruments

Electrochemical measurements were performed with a potentiostat/galvanostat Autolab model PGSTAT 30 (Eco Chemic, Utrecht, Netherlands) and a NOVA 1.7 software at laboratory temperature (25±1°C). The experimental conditions for electrochemical analysis included a three-electrode system consisting of a glassy carbon electrode with a surface area of 7.07 mm^2 as a working electrode, an Ag/AgCl (KCl 1.0 mol L^{-1}) reference electrode and a platinum wire counter electrode. The experiments were carried out in a 2.5 mL cylindrical cell. All the potentials were referred to an Ag/AgCl electrode. The pH measurements were done with a Metrohm model 691 pH/mV meter. The experimental conditions included a frequency between 100 kHz and 0.01 Hz, AC amplitude of 10 mV for EIS, and a scan rate of 100 mV s^{-1} for CV technique. All the experiments were carried out in 0.5 mmol L^{-1} $[Fe(CN)_6]^{3-/4-}$ (at a 1:1 molar ratio) as a redox probe in a 0.1 mol L^{-1} PBS solution. The obtained impedance spectra were represented as Nyquist plots and fitted by a Randles equivalent circuit. The UV-Vis spectra were obtained with an Optizen spectrophotometer model 3220, and the infrared spectra were achieved with an Equinox instrument model 55 Bruker. Scanning electron microscopy (SEM) and X-ray photoelectron spectroscopy (XPS) were performed respectively with a TESCAN instrument model VEGA3 and XPS 8025-BesTec (hν = 1486 eV) in vacuum < 10^{-7} Pa. The XPS peaks were deconvoluted by Gaussian/Lorentzian component after background subtraction.

2.3 Preparation and characterization of graphene nanosheets

Graphene nanosheets were prepared by oxidizing graphite using a new method and then reduced by hydrazine [21].The characterization of graphene oxide (GO) and reduced graphene oxide (RGO) had been investigated by UV-Vis spectra, infrared spectra (IR), scanning electron microscopy (SEM) and X-ray photoelectron spectroscopy (XPS) in our previous study [19]. Briefly, the prepared GO displayed a strong absorption band with a maximum at 228 nm and a shoulder at around 300 nm in the UV-Vis spectra, which are the characteristic bands of GO. A red shift of the main band to 273 nm indicated reduction upon hydrazine and formation of reduced graphene nanosheets.

The IR spectrum of graphene showed a $C-O$ stretch at 1222 cm^{-1}, a $O-H$ stretch at 3500-3300 cm^{-1}, and a $C=O$ stretch at 1720-1690 cm^{-1}. After reduction, the IR spectrum showed no peaks at 1720-1690 and 1222 cm^{-1}, which suggests removal of the epoxide and carboxyl groups on graphene. In any cases, as the results indicate, after reduction of GO by hydrazine, enough carboxylic acid groups remain on RGO in order to be grafted the DNA probes to the graphene surface [19]. The scanning electron microscopy (SEM) image of RGO showed a porous petal-like structure, which is generally expected to provide unique electrochemical properties with high activity due to the formation of a fraction of graphitic edge-plane defects combined with a large surface area.

The deconvoluted C1s peak of the X-ray photoelectron spectra (XPS) of RGO exhibited peaks centered at ~284.5 eV, ~285.5 eV, ~286.5, ~288.5 eV and ~289.3 eV attributed to sp^2-hybridized carbon atoms (C=C), carbon in aldehyde group (C–O), ether/epoxy group (C–O–C), carbonyl group (C=O) and carboxylic group (O–C=O), respectively. A calculation of the area percentage of RGO functional groups revealed that RGO contains a significant amount of COOH groups, allowing for a facile route of covalently grafting NH_2-DNA [19].

2.4 Fabrication of the electrochemical biosensor

Before fabrication, a non-modified GCE was polished by a 0.05 µm alumina slurry so that it got to be mirror-like, and then the mirror GCE was washed successively with anhydrous alcohol and water. This was followed by ultrasonication for 30 min in water and ethanol. 100 µL of a homogeneously dispersed solution of GNs (0.050 g mL^{-1}) was put onto the working electrode surface with a pipet and dried in ambient conditions. GNs can easily adhere to a GCE surface via interaction between graphene and GCE [19]. Next, NH_2-ssDNA probe was attached to the GNs modified electrode using EDC/NHS chemistry. The electrode was incubated in NH_2-ssDNA probe solution for 70 min at room temperature. To remove nonspecific adsorption of DNA, the electrode was kept in the solution Tween 20, (0.1%) for 55 min to displace nonspecifically bound oligonucleotides [22]. The DNA hybridization took place in complementary DNA in a phosphate buffer solution for 21 min at room temperature.

2.5 Genomic DNA extraction

The amelogenin gene was isolated from the blood samples using a DNA extraction kit (DNA fast Kit-Genfanavaran, Tehran, Iran).

PCR amplification of the genomic sample was performed using pairs of primers (5'-CCCTGGGCTCTGTAAAGAATAGTG-3' and 5'-ATCAGAGCTTAAACTGGGAAGCTG-3') of the amelogenin gene. PCR amplification was done in a final volume of 25 µL containing 100 ng total DNA as a template, 0.5 µL of each primers (10 pmol), 0.8 µL of $MgCl_2$ (50 mol L^{-1}), 0.5 µL of DNTP (10 mol L^{-1}), 2.5 µL of a 10X PCR buffer and 1.5 Units Taq DNA polymerase. The PCR was arranged based on the following conditions: initial denaturation at 94°C for 5 min followed by 35 cycles including denaturation at 94°C for 35 s, annealing at 62°C for 35 s, extension at 72°C 90 s and a final extension at 72°C for 5 min. The PCR products were electrophoresed on a 1.5% agarose gel and stained with ethidium bromide.

3. Results and discussion

3.1 Electrochemical characterization of the modified electrode

Compared with the other electrochemical methods, the impedance technique is investigated under stationary conditions as opposed to the wide potential windows used in CV. The impedance technique can provide more detailed information about the interfacial properties of surface-modified electrodes. In this experiment, two methods of EIS and CV were used to monitor the fabricating process of the biosensor, and the results are presented in Fig. 1. The impedance spectrum includes a semicircle portion at higher frequencies corresponding to the electron transfer limiting process and a linear part at low frequencies resulting from the diffusion limiting step of the electrochemical process. The diameter of the semicircle exhibits the R_{ct} of the layer, which points to its charge transfer behavior toward the redox couple. Thus, the semicircle diameter of EIS, which corresponds to R_{ct}, can be used to describe the interface properties of the electrode, and its increasing value exactly characterizes the immobilization for each step. The electron transfer of ferrocyanide through the modified electrode could be used as a valuable tool

to monitor the whole electrode fabrication process. Figure 1A shows the CVs of the electrode in 0.5 mM ferrocyanide ion for the modification steps of the electrode. The bare electrode indicated a pair of well-defined redox peaks with the anodic (E_{pa}) and cathodic (E_{pc}) peak potentials of 0.342 V and 0.253 V respectively, and a peak potential difference of 89 mV. These peaks could be definitely attributed to the redox behaviors of [$Fe(CN)_6^{3-/4-}$]. The graphene nanosheet modification increased the effective electrode surface area and the rate of electron transfer, which was evidenced by a slight increase in the cyclic voltammetric peak currents of [$Fe(CN)_6^{3-/4-}$] as compared to the bare electrode. By immobilizing the probe on the electrode surface, i_p decreased, indicating that the probe DNA was successfully immobilized on the surface of the modified electrode. The peak current decrease could be well assigned to the repellence of [$Fe(CN)_6^{3-/4-}$] by the negatively charged phosphate backbone of the DNA probe. When the hybridization of the modified electrode was proceeding with the target complementary DNA, the peak current of [$Fe(CN)_6^{3-/4-}$] was observed with a further decrease. The introduction of the complementary DNA increased the negative charge responsible for the increased repellence of the redox species. It was also discovered that the DNA immobilization and hybridization could be effectively done on the current fabricated electrode surface [23]. The impedance experiments for different modified electrodes were in good agreement with the results of the CV experiments. According to Fig. 1B, modification of the bare electrode with GNs led to the improvement of the electrode surface. This can be seen as a straight line which implies the characteristic of the diffusion limiting step of an electrochemical process. Because of the large surface area and the excellent conductivity of GNs, GNs-GCE shows less charge transfer resistance compared to GCE. A very small increase in R_{ct} after activation by a solution containing EDC/ NHS indicates the high conductivity of the modified electrode. In the later step, the immobilization of the probe generated an insulating DNA layer on the assembled surface, which significantly enlarged the diameter of the semicircle, implying a higher electron-transfer resistance. After being blocked with Tween, R_{ct} increased further in value, indicating displacement of nonspecifically bound oligonucleotides [19]. In the last step, hybridization of the DNA probe with the complementary DNA significantly enlarged the diameter of the semicircle in the impedance spectrum, implying a high electron transfer resistance caused by hybridization and more repulsion between the negative charge of the hybridized DNA and $[Fe(CN)_6]^{3-/4-}$ anions.

3.2 Optimization of biosensor conditions

Increasing the amount of the DNA probe immobilization on the electrode surface and its hybridization with the target DNA would markedly promote the detection ability of the DNA biosensor. Figure 2A shows the relationship of the DNA immobilization time on the efficiency of the biosensor. As it can be seen, the DNA probe was deposited onto GNs within the first 10 min. With further increase of the time, ΔR_{ct} (i.e. difference between the R_{ct} value of the probe DNA immobilized electrode and the R_{ct} value of blank) increased significantly, and the detection sensitivity can be amplified by the extension of time. However, when the immobilization time was more than about 70 min, ΔR_{ct} approached to saturation, in another word it started to level off after 70 min. Considering the largest ΔR_{ct}, an immobilization time of 70 min was selected for further studies. The effect of incubation in the Tween solution on the biosensor was also studied in Fig. 2B. Tween solution not only removes the nonspecifically adsorbed probe but also can fill the pinholes among the DNA monolayer [19]. ΔR_{ct} increased with an increase of time from 10 to 55 min and then reached a stable level. Therefore, the optimum time of incubation (55 min) was applied in the subsequent experiments. Our results also indicated that the detection sensitivity was critically related to the hybridization reaction time. As shown in Fig. 3A, the impedance values were a function of hybridization time. The best hybridization time for the 1.0×10^{-16} M solution of complementary DNA was found to be 21 min. Thus, 21 min was chosen as an optimum hybridization time for further experiments. The temperature of hybridization is an effective parameter in hybridization reactions. The results revealed that the ΔR_{ct} value increased with an increase of temperature up to about 47°C and rapidly decreased with an increase of temperature. The decrease of ΔR_{ct} at a high temperature was probably due to removal of some molecules from the electrode surface. Thus, 47°C was chosen as the optimum hybridization temperature (Fig. 3B).

3.3 Analytical performance

The fabricated biosensor was utilized to assay various concentrations of Amylogenin DNA. Figure 4, clearly demonstrates the CVs of the modified biosensor after incubation of this electrode in different concentrations of complementary DNA, over 10^{-18}–10^{-12} mol L^{-1}. By

increasing of the DNA concentration, the currents significantly decreased, but the peak potential separations (ΔE_p) increased. EIS plots were also obtained under the same conditions. As Fig. 5 shows, an increase in the DNA concentrations led to the rise of the interfacial charge transfer resistance, suggesting that, with an increase of the concentrations of the target, more sites of the surface were occupied by DNA molecules. The inset of Fig. 5 shows the relationship between the charge transfer resistance change (ΔR_{ct}) and the logarithm of the target concentrations for GNs-arrayed biosensor. Under the optimized conditions, the plot of the ΔR_{ct} versus the target concentration turned out to be made up of two linear segments. The first segment had a linear correlation to the target DNA concentration in the range of 1.0×10^{-20} to 1.0×10^{-14} mol L^{-1} with the regression equation of ΔR_{ct} =0.0686 Log C (mol L^{-1}) +2.0096 (R^2=0.9966), and the second segment resulted from 1.0×10^{-13} to 1.0×10^{-6} mol L^{-1} with the regression equation of ΔR_{ct} =0.022 Log C (mol L^{-1}) +1.305 (R^2 =0.992). The detection limit was estimated to be 7.1×10^{-21} (mol L^{-1}) based on $3s_b$. The performance of the current fabricated DNA biosensor was also carefully compared with those that were reported in the literature and used similar nanostructured materials for DNA immobilization layers. According to Table 1, the detection limit and the linear rang obtained in this study are extremely better than those in other studies.

3.4. Reproducibility and stability of the DNA sensor

The reproducibility of the DNA sensor was investigated by measuring the probe DNA modified electrode in the target DNA solution. Three parallel immobilizations of GNs were done on the GCE, activation was carried out by NHS/EDC, modification was made on the platform by 1.0×10^{-6} mol L^{-1} ssDNA, and then hybridization was performed with 1.0×10^{-16} mol L^{-1} target DNA. Three DNA sensors, made independently, showed the ΔR_{ct} values of 0.500, 0.495 and 0.532 KΩ with an acceptable variation coefficient of 3.93% (n=3). Thus, it emerged that a satisfactory reproducibility could be obtained by this system. The stability of ssDNA on the platform surface plays a critical role in obtaining good sensitivity. The stability of the modified electrode was also tested. No significant changes in the ΔR_{ct} values were observed for more than 10 times of EIS performance. In addition, when this modified electrode was stored in a 0.1 mol L^{-1} PBS buffer solution (pH 7.4) for at least one week at 25 °C, the electrode retained about 95% of its initial response.

3.5 Detection of real sample

Our biosensor was used for real sample analysis after extraction of DNA from blood samples by standard methods of DNA isolation [19]. The initial two genomic DNA samples (AMGY) were extracted from the blood using a commercial DNA extraction kit. Then, only one of those two samples was amplified by PCR. Afterwards, two distinct modified electrodes were incubated in these genomic DNA samples. Control experiments were performed with real samples when the probe was immobilized, and the real samples (AMGY) were used at the hybridization step. In the EIS results, R_{ct} of the dsDNA was compared with the original probe. The charge resistance difference ($\Delta R_{ct} = (R_{ct})_{\text{after hybridization}} - (R_{ct})_{\text{before hybridization}}$) was calculated as 2.34±0.41 kΩ for the sample genome without PCR and 8.84±1.56 kΩ for the PCR amplified sample. This significant difference in the ΔR_{ct} value between the probe ssDNA modified electrode and the hybridized electrode also confirmed that this biosensor is able to detect complementary sequence in real samples even without PCR.

In another part of the experiment, two genomic DNA samples (non-complementary, AMGX) were extracted from the blood of two persons and amplified using PCR. The PCR-amplified product was denatured by heating at 90^{o}C for 3 min and employed as the target. Initially, the ssDNA probe (AMGY) was immobilized on the two modified electrodes. EIS was recorded for the probe DNAs and R_{ct} was measured. Then, the modified electrodes were immersed in various genomic DNA samples. In the EIS results, R_{ct} of the dsDNA (non-complementary) was compared with the original probe. According to Table 2, the increase of R_{ct} was not noticeable as compared to the original probe. These results suggest that no hybridization reaction occurred between the probe and the non-complementary DNA.

3.6 DNA synthesis of amelogenin genes by DNA polymerase enzyme

To synthesize amelogenin DNA in the solution, initially the probes were immobilized on the surface of the modified electrode. Then, complementary oligonucleotides (PCR product) were introduced in order to hybridize onto the corresponding probe. Next, the electrode was immerged

in a solution containing 2 µL buffer, 2 µL Klenow enzyme (5U/ µL), 2 µL dNTP (5mmol/ µL) and 14 µL water at 37 ºC for 1 h until strain complementary DNA was fabricated according to the model. The electrode was then rinsed with D.I water. Consequently, for denaturation of dsDNA, the electrode was immersed in water at 93ºC for 5 min. As shown in Fig. 6, all the steps were followed by EIS.

In Fig. 6, curve a indicates the Nyquist plot of the modified electrode in a 5 mM solution of $[Fe(CN)_6]^{3-/4-}$. In this Fig., curve b shows the Nyquist plot of the electrode hybridized with the PCR product. Indeed, the increase in the R_{ct} value shows that ssDNA was hybridized with its complementary DNA sequence in the PCR product. For the detection method discussed in this paper, the available probe and the target oligonucleotide available in the PCR product (amelogenin fragment) must not have the same length. The PCR product is longer than ssDNA which has a part of the complementary sequence to hybridize with the ssDNA probe. The DNA polymerase enzyme (klenow fragment) caused the free nucleotides to be added in the solution (dNTP) along the probes. Curve c in Fig. 6 shows EIS after synthesis with the enzyme. The increase in R_{ct} demonstrates that the length of dsDNA was increased in the presence of the enzyme. Curve d of Fig. 6 shows the Nyquist plot of the electrode after denaturation. The decrease of the R_{ct} value demonstrates that dsDNAs were denatured and single strand structures were formed. The R_{ct} after denaturation was bigger than the R_{ct} of ssDNA because dsDNAs were denatured, the target DNAs were eliminated, and only the extended probes were maintained on the electrode surface. Hence, this suggests that the extended probe after synthesis was longer than the initial probe. It can be, thus, viewed as a confirmation of the synthesis of amelogenin genes by the enzyme along the probe.

4. Conclusion

Due to its fast performance and simple instrumentation, electrochemical detection of DNA is one of the best DNA detecting methods. In this paper, we described the set-up of a novel DNA label-free electrochemical biosensor for amylogenin detection, based on GNs matrices for DNA immobilization and hybridization. GNs-modified GCE could significantly increase the active sites and enhance the response signals during immobilization. A quite low detection limit (7.1×10^{-21} mol L^{-1}) indicated the improved performance of GNs-ssDNA composite materials. The linear detection range of the modified DNA electrode for the complementary 17-mer

oligonucleotide was achieved from 1.0×10^{-20} to 1.0×10^{-14} mol L^{-1} for the first segment and from 1.0×10^{-13} to 1.0×10^{-6} mol L^{-1} for the second segment. In principle, this system may be suitable not only for amylogenin in screening but also for real samples. The constructed DNA biosensor was established with a robust stability and a high level of reproducibility.

Acknowledgements

The authors wish to thank Yazd University Research Council for the financial support of this research.

[1] J.M. Butler, Genetics and Genomics of Core Short Tandem Repeat Loci Used in Human Identity Testing, J. Forensic Sci. 51(2006) 253–265.

[2] S. Reisberga, B. Piroa, V. Noela, M.C. Pham, Selectivity and sensitivity of a reagentless electrochemical DNA sensor studied by square wave voltammetry and fluorescence, Bioelectrochem. 69(2006) 172–179.

[3] C. Luo, H. Tang, W. Cheng, L. Yan, D. Zhang, H. Ju, S. Ding, A sensitive electrochemical DNA biosensor for specific detection of Enterobacteriaceae bacteria by Exonuclease III-assisted signal amplification, Biosens. Bioelectron. 48(2013) 132-137.

[4] D. Gerion, F. Chen, B. Kannan, A. Fu, W.J. Parak, D.J. Chen, A. Majumdar, A.P. Alivisatos, Room-temperature single-nucleotide polymorphism and multiallele DNA detection using fluorescent nano crystals and microarray, Anal. Chem. 75(2003) 4766–4772.

[5] N.L. Rosi, C.A. Mirkin, Nanostructures in biodiagnostics, Chem. Rev. 105(2005)1547–1562.

[6] L. He, M.D. Musick, S.R. Nicewarner, F.G. Salinas, S.J. Benkovic, M.J. Natan, C.D. Keating, Colloidal Au-enhanced surface plasmon resonance for ultrasensitive detection of DNA hybridization, J. Am. Chem. Soc. 122(2000) 9071–9077.

[7] T.G. Drummond, M.G. Hill, J.K. Barton, Electrochemical DNA sensors, Nat. Biotechnol. 21(2003) 1192–1199.

[8] R.J. Lao, S.P. Song, H.P. Wu, L.H. Wang, Z.Z. Zhang, L. He, C.H. Fan, Electrochemical interrogation of DNA monolayers on gold surfaces, Anal. Chem. 77(2005) 6475–6480.

[9] C.F. Ding, F. Zhao, M.L. Zhang, S.S. Zhang, Hybridization biosensor using 2, 9-dimethyl-1, 10-phenantroline cobalt as electrochemical indicator for detection of hepatitis B virus DNA, Bioelectrochem. 72(2008) 28–33.

[10] A.K. Geim, K.S. Novoselov, The rise of graphene, Nat. Mater. 6(2007) 183-191.

[11] R.F. Service, Carbon sheets an atomic thick give rise to graphene dreams, Science 324(2009) 875-877.

[12] K.S. Novoselov, A.K. Geim, S.V. Morozov, D. Jiang, Y. Zhang, S.V. Dubonos, I.V. Grigorieva, A.A. Firsov, Electric field effect in atomically thin carbon films, Science 306(2004) 666–669.

[13] M. Chi, Y.P. Zhao, First principle study of the interaction and charge transfer between graphene and organic molecules, Comput. Mater. Sci. 56(2012) 79–84.

[14] Y.Y. Choi, S.J. Kang, H.K. Kim, W.M. Choi, S.I. Na, Multilayer graphene films as transparent electrodes for organic photovoltaic devices, Sol. Energy Mater. Sol. Cells 96(2012) 281–285.

[15] B. Zhang, Q. Li, T.H. Cui, Ultra-Sensitive suspended graphene nanocomposite cancer sensors with strong suppression of electrical noise, Biosens. Bioelectron. 31(2012) 105–109.

[16] Y. Chen, X. Zhang, P. Yu, Y. Ma, Electrophoretic deposition of graphene nanosheets on nickel foams for electrochemical capacitors, J. Power Sources 195 (2010) 3031–3035.

[17] P.C. Lian, X.F. Zhu, H.F. Xiang, Z. Li, W.S. Yang, H.H. Wang, Enhanced cycling performance of Fe_3O_4–graphene nanocomposite as an anode material for lithium-ion batteries, Electrochim. Acta 56(2010) 834–840.

[18] J.Y. Park, S.M. Park, DNA Hybridization Sensors Based on Electrochemical Impedance Spectroscopy as a Detection Tool, Sensors 9(2009) 9513-9532

[19] A. Benvidi, N. Rajabzadeh, M. Mazloum-Ardakania, M.M. Heidari, A. Mulchandani, Simple and label-free electrochemical impedance Amelogenin gene hybridization biosensing based on reduced graphene oxide, Biosens. Bioelectron. 58(2014) 145-152.

[20] B.L. Jensen, S. Kreiborgs, Craniofacial abnormalities in 52 schoolage and adult patients with cleidocranial dysplasia, J Craniofac Genet Dev Biol. 13(1993) 259-269.

[21] D.C. Marcano, D.V. Kosynkin, J.M. Berlin, A. Sinitskii, Z. Sun, A. Slesarev, L.B. Alemany, W. Lu, M. Tour, Improved Synthesis of Graphene Oxide, ACS Nano 4(2010) 4806–4814.

[22] P.H. Rogers, E. Michel, C.A. Bauer, S. Vanderet, D. Hansen, B.K. Roberts, A. Calves, J.B. Crews, K.O. Lau, A. Wood, D.J. Pine, P.V. Schwartz, Selective, controllable and reversible aggregation of polystyrene latex microspheres via DNA hybridization, Langmuir 21(2005) 562-5569.

[23] O. Akhavan, E. Ghaderi, R. Rahighi, Toward Single-DNA Electrochemical Biosensing by Graphene Nanowalls, ACS Nano 6(2012) 2904-2916.

[24] A.L. Liu, G.X. Zhong, J.Y. Chen, S.H. Weng, H.N. Huang, W. Chen, L.Q. Lin, Y. Lei, F.H. Fu, Z.L. Sun, X.H. Lin, J.H. Lin, S.Y. Yang, A sandwich-type DNA biosensor based on electrochemical co-reduction synthesis of graphene-three dimensional nanostructure gold nanocomposite films, Anal. Chim. Acta 767(2013) 50-58.

[25] T. Yang, Q. Li, X. Li, X. Wang, M. Du, K. Jiao, Freely switchable impedimetric detection of target gene sequence based on synergistic effect of ERGNO/PANI nanocomposites, Biosens. Bioelectron. 42(2013) 415–418.

[26] Y. Du, S. Guo, S. Dong, E. Wang, An integrated sensing system for detection of DNA using new parallel-motif DNA triplex system and graphene--mesoporous silica--gold nanoparticle hybrids, Biomater. Sci. 32(2011) 8584-8592.

[27] Y. Hu, F. Li, D. Han, T. Wu, Q. Zhang, L. Niu, Y. Bao, Simple and label-free electrochemical assay for signal-on DNA hybridization directly at undecorated graphene oxide, Anal. Chim. Acta 753(2012) 82-89.

Figure captions

Fig. 1. (A) The cyclic voltamograms of the electrode in 0.5 mM $[Fe(CN)_6]^{3-/4-}$ for different steps of modification and (B) EIS measurements were made in $[Fe(CN)_6]^{3-/4-}$ (0.5×10^{-3} mol L^{-1}; 1:1) as a redox probe, at a constant DC potential of +0.2 V for the steps of biosensor modification.

Fig. 2. (A) The optimization of the time of probe immobilization. Inset: comparison of the signal intensities versus the consumed time for the probe self- assembly. The error bars correspond to the ±1 standard deviation. (B) The optimization of the incubation time of the ssDNA immobilized electrode in the Tween solution (0.1 %). Inset: comparison of the signal intensities versus the incubation time in the Tween solution.

Fig. 3. (A) The optimization of the hybridization time. Inset: comparison of the signal intensities versus the hybridization time. (B) The optimization of temperature for the hybridization. Inset: comparison of the signal intensities versus the temperature for the hybridization.

Fig. 4. CVs recorded at the ssDNA immobilized on the modified electrode and after hybridization with its complementary with different concentrations. Inset: plot of the dependence of ΔI_p versus the logarithm concentration of target.

Fig. 5. Nyquist diagrams recorded at the ssDNA immobilized and after hybridization with its complementary with different concentrations. Inset (A): The equivalent circuit used to process the impedance data in the presence of redox couples, R_1 (electrolyte solution resistance), R_2 (element of interfacial electron transfer resistance) CPE_1 (constant phase element), W_{01} (Warburg impedance resulting from the diffusion of ions). Each point is the mean of measurements from 3 independent biosensors, and the error bars correspond to the ±1 standard deviation. Insets (B, C and D): Plot of the dependence of ΔRct versus the concentration of the target DNA.

Fig. 6. Nyquist diagrams recorded at a) GCE/RGO/ss-DNA, b) GCE/RGO/ss-DNA hybridized with PCR product, c) GCE/RGO/ds-DNA after synthesis and d) GCE/RGO/ds-DNA after denaturation.

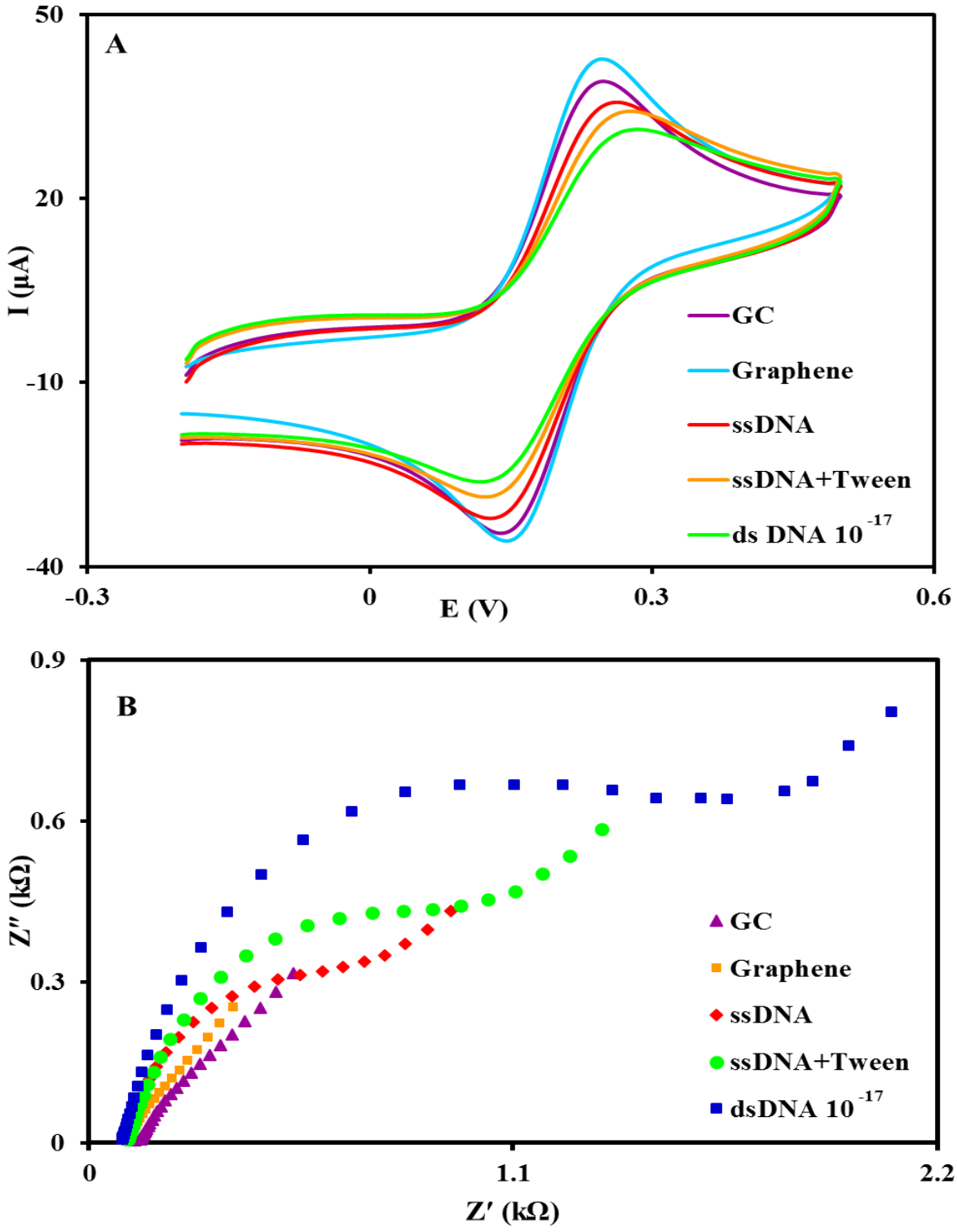

Fig. 1

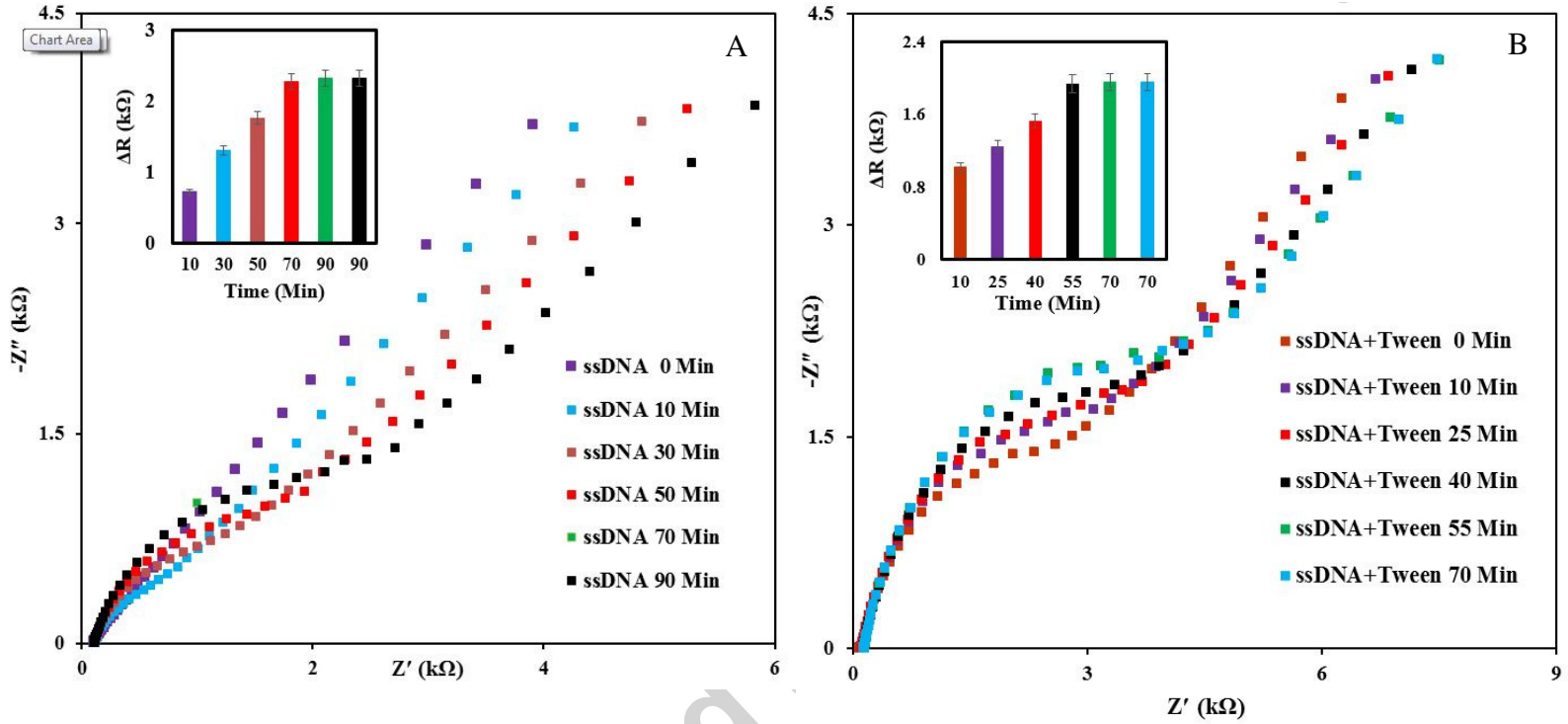

Fig. 2

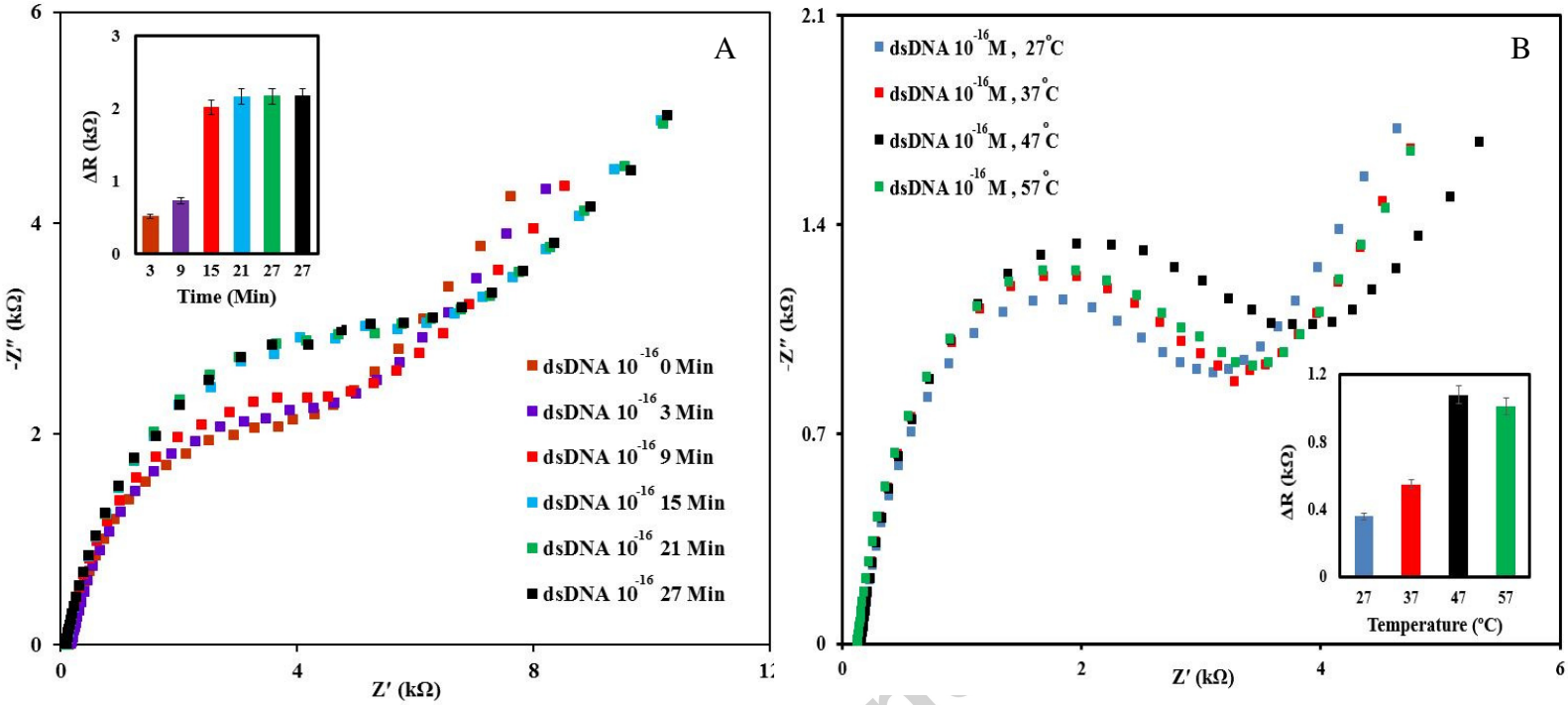

Fig. 3.

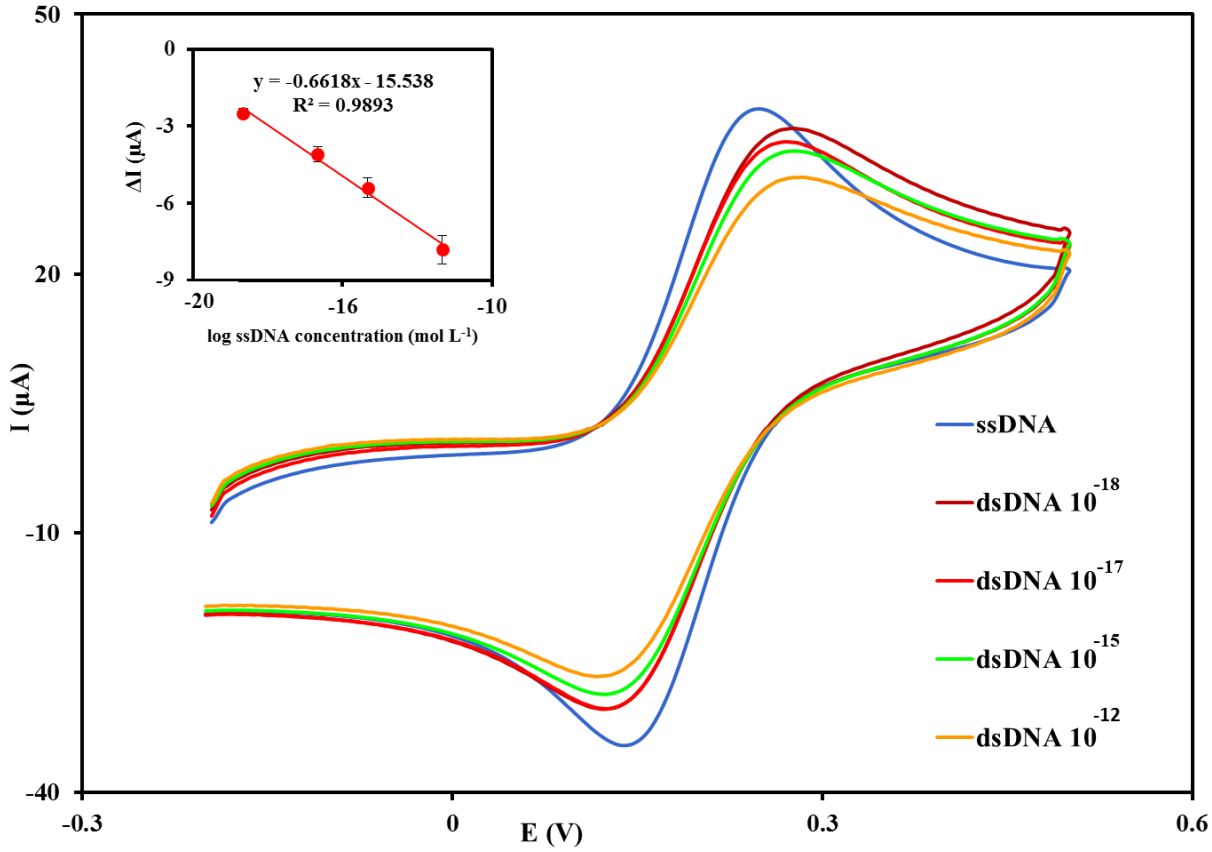

Fig. 4

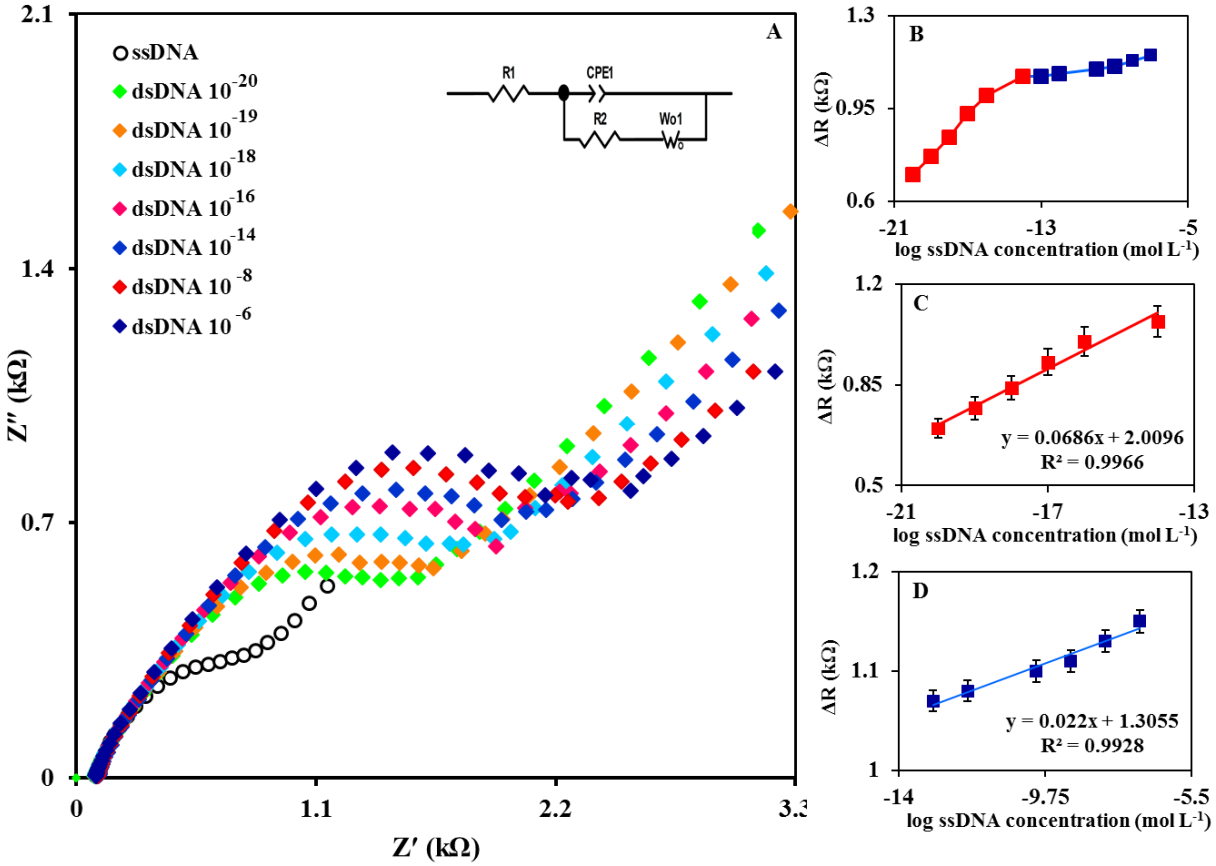

Fig. 5

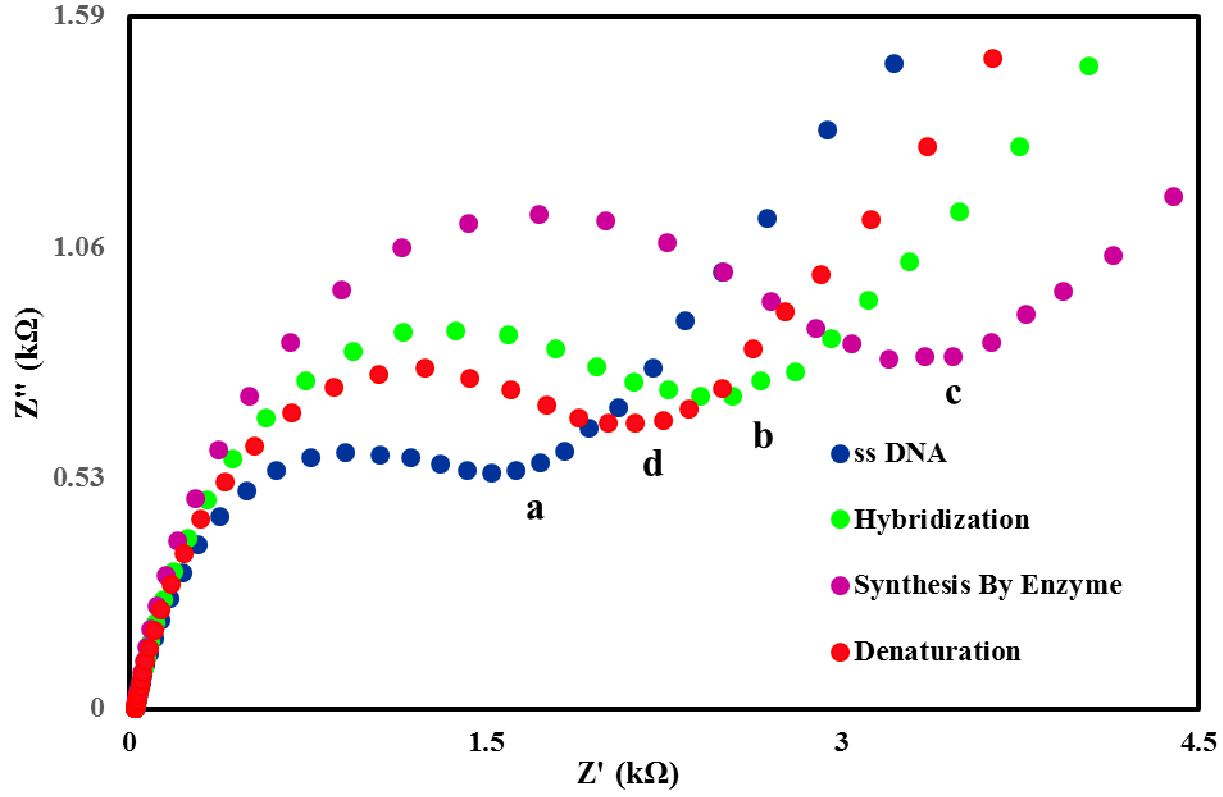

Fig. 6

Table 1. Comparison of the proposed sensor with other ones for specific DNA sequence hybridization detection

Electrode	Modifier	Dynamic range (mol L^{-1})	Limit of detection (mol L^{-1})	Reference
GCE	RGNW	1.0×10^{-16} - 1.0×10^{-2}	9.4×10^{-18}	[23]
GCE	RGNS	2.0×10^{-12} - 1.0×10^{-2}	5.4×10^{-15}	[23]
GCE	Graphene-nanostructure gold	5.0×10^{-14} - 5.0×10^{-12}	3.4×10^{-15}	[24]
GCE	graphene oxide	1.0×10^{-15} - 1.0×10^{-8}	2.5×10^{-16}	[25]
ITO	Graphene- Silica-gold	1.0×10^{-14} - 1.0×10^{-10}	1.0×10^{-15}	[26]
GCE	graphene oxide	1.0×10^{-12} - 1.0×10^{-6}	1.1×10^{-13}	[27]
GCE	Reduced graphene oxid	1.0×10^{-20} -1.0×10^{-14}	3.2×10^{-21}	[19]
GCE	Reduced graphene oxid	1.0×10^{-20} -1.0×10^{-14} 1.0×10^{-13} -1.0×10^{-6}	7.1×10^{-21}	This work

Reduced graphene nanowalls

Reduced graphene nanosheet

Table 2. The mean of R_{ct} (kΩ) for the two DNA probes and hybridization with its noncomplementary strain (dsDNA) in the genome sample by EIS. Each measurement was repeated for at least 3 times.

Electrode	R_{ct} (kΩ) Probe DNA	R_{ct} (kΩ) dsDNA	ΔR_{ct} (kΩ)
1	1.28 (±0.12)	1.34 (±0.10)	0.06
2	1.41 (±0.09)	1.55 (±0.09)	0.11

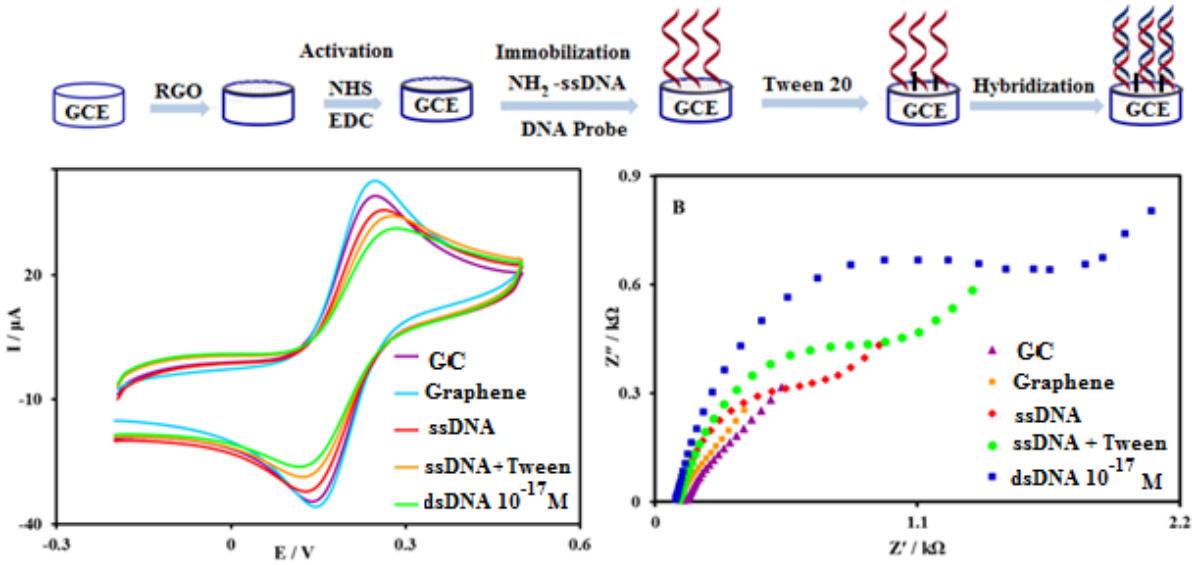

Highlights:

- A simple and label-free biosensor based on GNs for detection of Amylogenin DNA.
- The biosensor shows a high level of stability and reproducability.
- This DNA biosensor can detect the target DNA with a detection limit of 7.1×10^{-21} M.

A copy of a nucleic acid was synthesized at the electrode surface and detected by EIS.